Wireless Pers Commun (2017) 96:1871–1885
DOI 10.1007/s11277-017-4273-5

Cooperative Spectrum Sensing with Small Sample Size in Cognitive Wireless Sensor Networks

Shaoyang Men[1] · Pascal Chargé[1] · Sébastien Pillement[1]

Published online: 26 April 2017

Abstract Cooperative spectrum sensing based on Dempster–Shafer (D–S) theory has attracted a large amount of interest in cognitive wireless sensor networks. However, most of them employ energy detection (ED) in local sensing, where the classical Gaussian approximation of ED is accurate only with a large number of data samples. In this paper, aiming at drastically reduce the computational cost and the sensing process duration, we consider that a small sample size is collected at each node of the network. In this configuration, to perform the D–S fusion we introduce new basic probability of assignment functions derived from the statistics of the eigenvalues of the samples covariance matrix. To that end, we introduce a relevant approximation of the Tracy–Widom distribution that allows us to cope with the small sample size. Simulation results show that the proposed method allows to improve significantly the detection performance compared to other techniques, even with small number of samples.

Keywords Spectrum sensing · Eigenvalue · Random matrix theory · Dempster–Shafer theory · Cognitive wireless sensor networks

1 Introduction

Nowadays, cognitive radio (CR) technology has been widely applied to wireless sensor networks (WSNs), in order to create the promising infrastructures CWSNs. As the first step of CR, spectrum sensing (SS) is one of the key enabling technology for preventing hazardous interferences with the licensed users (Primary User, PU) and identifying the available spectrum. A lot of SS techniques [1], which mainly include matched filtering [2], energy detector [3], cyclostationary feature detection [4] and waveform-based sensing [5],

✉ Shaoyang Men
shaoyang.men@univ-nantes.fr

[1] UBL, UMR CNRS 6164, IETR Laboratory, University of Nantes, Nantes, France

have been proposed. Among all these methods, energy detection (ED) is an engaging technique for CWSNs applications, due to its low amount of computational power requirements and blind detection characteristics [6]. However, radio channel conditions practically experienced by the cognitive users (or secondary users, SU), i.e. path loss, multipath, shadowing due to obstacles and possibly non-line-of-sight between SU and PU, make it difficult for a SU to make a decision only on its own measurement. It is thus obvious that a stand-alone decision about the fact that a PU is emitting or not, made independently by each SU, is not reliable enough. In that context it is much more preferable to use a cooperative spectrum sensing (CSS) strategy.

Cooperative spectrum sensing has attracted a lot of attention [7, 8] and has been shown to be an effective technique to improve the detection performance by exploiting spatial diversity. Several distributed SU in an area are then cooperatively involved in the spectrum sensing, which allows to mitigate the channel effects. A fusion center (FC) is then in charge of merging information collected by the SU and making a final decision about the spectrum occupancy. Unfortunately cooperative sensing can incur additional work and cost; i.e. delay, fusion processing and overhead transmissions. In order to mitigate the impact of these issues, and not to increase the overall computation cost of the CSS process at an unbearable level, a part of the solution is to reduce the sample size at each SU. In particular it reduces the sensing time and saves energy.

Recently, in order to effectively combine the information from different SU, Dempster–Shafer (D–S) theory of evidence has been applied into cooperative spectrum sensing in order to make a reliable decision [9–12]. In [9], the credibility of the channel condition between PU and SU is quantified by the basic probability assignment (BPA) estimation and D–S theory of evidence is firstly applied into FC in order to fuse the different detection from each SU. That turns out to be better than the traditional logic fusion “And” and “Or” rules. The authors in [10] reduce the reporting bandwidth and keep the performance by utilizing special characteristics of hypothesis and employing the Lloyd-Max quantization method. In [11], an enhanced D–S theory cooperative spectrum sensing algorithm is proposed against spectrum sensing data falsification attack by removing the lowest reliable SU, which is evaluated by considering the Max-Min similarity degree between any two SUs. Finally, [12] evaluates the trustworthiness degree from the current and historical aspects and establishes a “soft update” approach for the reputation value maintenance in order to obtain better detection performance.

However, these existing cooperative spectrum sensing algorithms based on D–S theory of evidence, called the traditional D–S (T-DS) fusion [9], employ energy detection in their local sensing process to construct BPA functions, where the classical Gaussian approximation of ED is accurate only when the number of samples is high [13]. As mentioned above, however, when CSS is expected to get as energy-efficient as possible, a significant reduction of sample size at each SU would be worthwhile. Thus in this work, we propose to replace the traditional ED technique with a sensing principle in accordance with the small sample size requirement. Recently some spectrum sensing techniques based on the eigenvalue analysis of the samples convariance matrix [14–17] have exhibited appealing performance. Among them, [14] makes use of the statistics of the largest eigenvalue of the covariance matrix of the observation, which is a Tracy–Widom law. Since our ambition is to massively reduce the number of samples used for the spectrum detection, we introduce an appropriate approximation of the Tracy–Widom distribution to characterize the largest eigenvalue in the very small sample size case [18]. Then in this paper we propose an effective cooperative spectrum sensing scheme with small sample size in CWSNs. As will be explained in Sect. 3, the advantage of the proposed technique compared to other eigenvalue-based spectrum sensing techniques [14–17] is that we form a thin observation matrix according to a more reasonable Tracy–Widom approximation, which allows to get a small dimension covariance matrix. That makes a big difference with the other methods in terms of computation cost. We also propose a new BPA function based on the largest eigenvalue of the received sample covariance matrix, which considers the credibility of local spectrum sensing and is applied to the D–S theory of evidence. Finally, a more reliable final decision is made. Simulation results verify the effectiveness of the proposed method for small sample size scenarios.

The remainder of the paper is organized as follows. In Sect. 2, the local SS system model based on the covariance matrix of received signal is proposed, and D–S theory of evidence is presented. The proposed cooperative spectrum sensing scheme with small sample size is presented in Sect. 3, where a suited Tracy–Widom approximation is introduced and a thin observation matrix is formed, then new BPA functions are constructed at the local sensing side, and finally the D–S fusion is applied at the FC. Simulations and conclusions are respectively presented in Sects. 4 and 5.

2 Local SS System Model and D–S Theory of Evidence

In our CSS scheme, we consider a centralized CSS based on D–S theory of evidence. As shown in Fig. 1, the CSS scenario in CWSNs includes one PU, one FC and N_{su} SUs where each SU is equipped with one receive antenna. Then, each SU senses the channel and sends the acquired information to the FC. This latter makes a final decision and returns the results to each SU. In detail, Fig. 1 shows the CSS framework where spectrum sensing is periodically executed before data transmissions [10]. Firstly SU receives the sensing request from the FC and measures the channel, then each SU reports its sensing or processed information to the FC, finally the FC makes a decision whether the PU is present or not, and broadcasts the result to each SU. Therefore, in the following we will present the system model in local sensing at SU and the D–S theory of evidence implemented at the FC.

2.1 Local SS System Model

Some notations used in this paper are listed as follows: superscript T and $\dagger$ stand for transpose and Hermitian (transpose-conjugate), respectively. We use boldface lower case letters for column vectors and boldface capital letters for matrices.

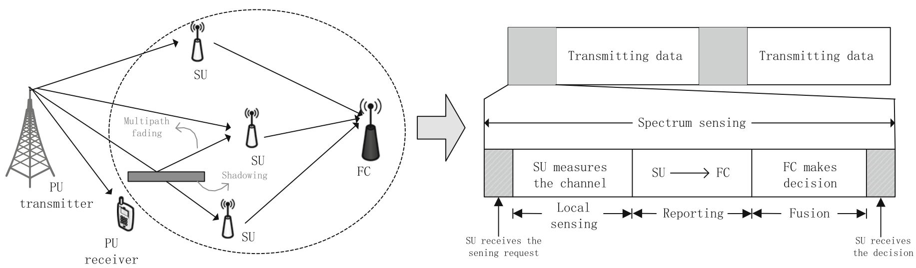

Fig. 1 Scenario and framework of cooperative spectrum sensing in CWSNs

For presentation convenience and without loss of generality, we consider the local spectrum sensing with a discrete model at SU. Then, spectrum sensing can be formulated as a binary hypothesis test between the following two hypotheses:

$$H_0: \quad x(nT_s) = \eta(nT_s) \tag{1}$$

$$H_1: \quad x(nT_s) = \boldsymbol{h}^T \boldsymbol{s}(nT_s) + \eta(nT_s) \tag{2}$$

where T_s is the sampling period, $x(nT_s)$ is the received signal at a SU, $\boldsymbol{h} = [h(0), h(T_c), \ldots, h((N_c - 1)T_c)]^T$ stands for N_c taps of the multipath discrete channel impulse response which includes the transmission filter, the channel itself and the receiver filter, $N_c T_c = T_h$ being the maximum length of the impulse response. Here, we consider that the received signal of a SU is sampled at a low rate $T_s > T_h$ (under-sampling). For practicality and without loss of generality, we consider the channel $\boldsymbol{h}$ as the Clarke's Rayleigh fading model which is a baseline filtered white Gaussian noise (FWGN) model [19, 20]. In the Clarke model, isotropic scattering and linear relationship between input and output are assumed, and it includes two branches, one for a real part and the other for an imaginary part. The random process of Clarke's fading model with N_m multipaths can be described as the sum-of-sinusoid as follows:

$$h_I(lT_c) = \frac{1}{\sqrt{N_m}} \sum_{i=1}^{N_m} \cos\left\{ 2\pi f_D \cos\left[\frac{(2i-1)\pi + \theta}{4N_m} \right] lT_c + \alpha_i \right\} \tag{3}$$

$$h_Q(lT_c) = \frac{1}{\sqrt{N_m}} \sum_{i=1}^{N_m} \sin\left\{ 2\pi f_D \sin\left[\frac{(2i-1)\pi + \theta}{4N_m} \right] lT_c + \beta_i \right\} \tag{4}$$

$$h(lT_c) = h_I(lT_c) + jh_Q(lT_c) \tag{5}$$

where θ, α_i and β_i are uniformly distributed over [0, 2π) for all l and are mutually distributed, f_D is the maximum Doppler spread. $\boldsymbol{s}(nT_s) = [s(nT_s), s(nT_s - T_c), \ldots, s(nT_s - (N_c - 1)T_c)]^T$ is the discrete model of the PU signal. The noise signal $\eta(nT_s)$ is assumed to be complex white Gaussian with zero mean and σ_η^2 variance. Furthermore, it is assumed that noise and signal are uncorrelated.

In order to create a covariance matrix of observations, each SU collects N_s frames $\boldsymbol{x}_{i=0,1,\ldots,N_s-1}$ of L consecutive samples which is a stationary random vector. As shown in the next section, the local spectrum sensing operation can rely on the eigenvalue decomposition of this matrix. Then the following matrices can be defined:

$$\mathbf{X} \stackrel{\text{def}}{=} [\boldsymbol{x}_\mathbf{0}, \boldsymbol{x}_\mathbf{1}, \ldots, \boldsymbol{x}_\mathbf{i}, \ldots, \boldsymbol{x}_{\mathbf{N_s-1}}] \tag{6}$$

$$\mathbf{S} \stackrel{\text{def}}{=} [\boldsymbol{s}_\mathbf{0}, \boldsymbol{s}_\mathbf{1}, \ldots, \boldsymbol{s}_\mathbf{i}, \ldots, \boldsymbol{s}_{\mathbf{N_s-1}}] \tag{7}$$

$$\boldsymbol{\eta} \stackrel{\text{def}}{=} [\boldsymbol{\eta}_0, \boldsymbol{\eta}_1, \ldots, \boldsymbol{\eta}_i, \ldots, \boldsymbol{\eta}_{N_s-1}] \tag{8}$$

where, $\boldsymbol{x}_i$, $\boldsymbol{s}_i$, and $\boldsymbol{\eta}_i$ respectively denote the $L \times 1$ received random vector, the $LN_c \times 1$ PU signal vector $\boldsymbol{s}_i = [\boldsymbol{s}(iLT_s)^T \boldsymbol{s}((iL+1)T_s)^T \ldots \boldsymbol{s}(((i+1)L-1)T_s)^T]^T$, and the $L \times 1$ random noise vector.

When there is no PU emitting

$$\boldsymbol{x}_i = \boldsymbol{\eta}_i \tag{9}$$

When a PU is present,

$$\boldsymbol{x}_i = \begin{bmatrix} x(iLT_s) \\ x((iL+1)T_s) \\ \vdots \\ x(((i+1)L-1)T_s) \end{bmatrix} \tag{10}$$

$$= \begin{bmatrix} \boldsymbol{h}_1^T \boldsymbol{s}(iLT_s) + \eta(iLT_s) \\ \boldsymbol{h}_2^T \boldsymbol{s}((iL+1)T_s) + \eta((iL+1)T_s) \\ \vdots \\ \boldsymbol{h}_L^T \boldsymbol{s}(((i+1)L-1)T_s) + \eta(((i+1)L-1)T_s) \end{bmatrix} \tag{11}$$

$$= \mathbf{H_i}\boldsymbol{s}_\mathbf{i} + \boldsymbol{\eta}_\mathbf{i} \tag{12}$$

where $\mathbf{H_i}$ is a $L \times LN_c$ channel matrix defined as:

$$\mathbf{H_i} \overset{\text{def}}{=} \begin{bmatrix} \boldsymbol{h}_\mathbf{1}^\mathbf{T} & \boldsymbol{0} & \cdots & \boldsymbol{0} \\ \boldsymbol{0} & \boldsymbol{h}_\mathbf{2}^\mathbf{T} & \cdots & \boldsymbol{0} \\ \vdots & \vdots & \ddots & \vdots \\ \boldsymbol{0} & \boldsymbol{0} & \cdots & \boldsymbol{h}_\mathbf{L}^\mathbf{T} \end{bmatrix} \tag{13}$$

Statistical covariance matrix of the received signal, the PU signal and the noise can be respectively defined as:

$$\mathbf{R_X} = \mathrm{E}[\boldsymbol{x}_\mathrm{i}\boldsymbol{x}_\mathrm{i}^\dagger] \tag{14}$$

$$\mathbf{R_S} = \mathrm{E}[\mathbf{H_i}\boldsymbol{s}_\mathbf{i}\boldsymbol{s}_\mathbf{i}^\dagger\mathbf{H}_\mathbf{i}^\dagger] \tag{15}$$

$$\mathbf{R}_\eta = \mathrm{E}[\boldsymbol{\eta}_\mathrm{i}\boldsymbol{\eta}_\mathrm{i}^\dagger] \tag{16}$$

where $\boldsymbol{x}_i$, $\boldsymbol{s}_i$ and $\boldsymbol{\eta}_i$ are assumed to be zero-mean stochastic stationary processes.

Then the binary hypothesis, (1) and (2), can be rewritten in a matrix form as

$$H_0: \quad \mathbf{R_X} = \mathbf{R}_\eta \tag{17}$$

$$H_1: \quad \mathbf{R_X} = \mathbf{R}_S + \mathbf{R}_\eta \tag{18}$$

However, in practice we only can get a finite number of samples. Thus, the sample covariance matrix $\mathbf{R_X}$ can be estimated as

$$\hat{\mathbf{R}}_\mathbf{X} = \frac{1}{N_s}\mathbf{X}\mathbf{X}^\dagger \tag{19}$$

As mentioned previously, noise is a white Gaussian process. In case of the presence of a PU, whose signal is obviously not correlated to the noise, the sampling period has been set sufficiently large ($T_s > T_h$) to assume that the observation samples $\mathbf{X}$ are independent and identically distributed random variables. Then in the H_0 case (no PU), the mean power of the observed signal $\mathbf{X}$ is given by the noise power $P = \sigma_\eta^2$, and in the H_1 case (a PU is present) the theoretical mean power samples is $P = \sigma_s^2 + \sigma_\eta^2$ where σ_s^2 is the received PU signal power through the channel.

2.2 D–S Theory of Evidence

The Dempster–Shafer theory of evidence, which was first introduced by Dempster and was later extended by Shafer [21], is a mathematical theory of evidence which allows to combine evidence from different sources and evaluate the credibility of a system state.

According to the D–S theory of evidence, in our spectrum sensing context let $\Omega = \{H_0, H_1\}$ be the set representing all possible states of the system under consideration, called the frame of discernment. Then 2^Ω is the set of all subsets of Ω, including the empty set $\emptyset$. In our framework, $2^\Omega = \{\emptyset, \{H_0\}, \{H_1\}, \Omega\}$. Each $\mathrm{SU_i}$ is a source of information and will provide a set of elementary evidences. For each $\mathrm{SU_i}$, due to stochastic characteristics of communication channel, there is uncertainty in local spectrum sensing results. Thus, the theory of evidence allows to assign a belief mass to each element of the set 2^Ω for managing uncertainty. This mass is also defined as a basic probability assignment function (BPA) m_i from 2^Ω to [0, 1]. It has two properties:

$$m_i(\emptyset) = 0, \quad \text{and} \quad \sum_{\mathrm{B_j} \subset 2^\Omega} \mathrm{m_i(B_j)} = 1 \tag{20}$$

where the mass $m_i(B_j)$ represents the belief that “ the $\mathrm{CU_i}$ is estimating that the event B_j is true ”, and $B_j \subset 2^\Omega$.

After evaluating the reliability of each $\mathrm{SU_i}$ detection, we need to make a final decision whether PU is present or not based on each $\mathrm{SU_i}$ information. Then, according to D–S rule of combination [21], the mass functions from different $\mathrm{SU_i}$ $m_i(i = 1, \ldots, N_{su})$ are combined and a new mass function $m(B_d)$ is obtained as:

$$\begin{aligned} m(B_j) &= (m_1 \oplus m_2 \oplus \cdots \oplus m_{N_{su}})(B_j) \\ &= \frac{1}{1-\kappa} \sum_{B_1 \cap B_2, \ldots, B_{N_{su}} = B_j} \prod_{i=1}^{N_{su}} m_i(B_i) \end{aligned} \tag{21}$$

$$\kappa = \sum_{B_1 \cap B_2, \ldots, B_{N_{su}} = \emptyset} \prod_{i=1}^{N_{su}} m_i(B_i). \tag{22}$$

where κ is interpreted as a measure of conflict among the different SU and is introduced as a normalization factor.

3 Proposed Small-Sample-Size D–S Theory CSS

The proposed CSS strategy relies on a fusion process using the D–S theory and a new set of basic probability assignments (BPA, given in the next section). BPA definition and evaluation is the key point of the D–S fusion. In most applications, it is generally assumed that a sufficiently large number of samples is available in order to correctly estimate BPAs and perform a reliable fusion. But in this work, we consider that the SU are very limited in terms of sample size. Following the success of the utilization of the D–S fusion [21] in CSS, we propose to define a new reliable BPA by using eigenvalues of the covariance matrix of the observation enabling to have a small number of collected samples.

3.1 Largest Eigenvalue Analysis

Whether a PU signal is present or not in the collected samples at a SU, according to the statistical properties of the samples, the observation covariance matrix $\hat{\mathbf{R}}_{\mathbf{X}}$ in (19) can be considered as a Whishart matrix [22]. In such a case, according to [23] when the number of samples is high enough, the largest eigenvalue of the matrix $\mathbf{R}_{\mathbf{X}}$ is ruled by the Tracy–Widom distribution. Parameters of the distribution can be defined as functions of N_s and L, the dimensions of the observation matrix $\mathbf{X}$. The following theorem allows to establish the parameters of the Tracy–Widom distribution in the asymptotical case (or when the number of samples is large).

Theorem 1 *Assume that the received signal is real. Let* $\mathbf{A} = \frac{\mathbf{N_s}}{\mathbf{P}}\hat{\mathbf{R}}_{\mathbf{X}}$, $\phi = (\sqrt{N_s - 1} + \sqrt{L})^2$, *and* $\upsilon = (\sqrt{N_s - 1} + \sqrt{L})(1/\sqrt{N_s - 1} + 1/\sqrt{L})^{1/3}$. *Then,* $\frac{\lambda_1(\mathbf{A}) - \phi}{\upsilon}$ *converges to the Tracy–Widom distribution of order 1* (W_1) [23].

Reducing the number of samples (small $N_s \times L$ product) means that definitions of $\phi(N_s, L)$ and $\upsilon(N_s, L)$ in Theorem 1 are no longer correct. Recently in [18] it has been found that when facing with thin observation matrix X, namely when L is as small as 2, more appropriate parameters of the Tracy–Widom distribution should be chosen. Then, according to [18] when L is very small, and referring to the theorem, the largest eigenvalue λ_1 is considered to be ruled by the Tracy–Widom distribution of order 1, with the following mean and variance parameters :

$$\mu = \frac{P}{N_s}\left(\sqrt{N_{s-}} + \sqrt{L_-}\right)^2 \tag{23}$$

$$\sigma^2 = \left(\frac{P}{N_s}\right)^2\left(\sqrt{N_{s-}} + \sqrt{L_-}\right)^2\left(\frac{1}{\sqrt{N_{s-}}} + \frac{1}{\sqrt{L_-}}\right)^{2/3} \tag{24}$$

where $N_{s-} = N_s - \frac{1}{2}$ and $L_- = L - \frac{1}{2}$. In (23) and (24) the mean power P is respectively equal to σ_η^2 or $\sigma_s^2 + \sigma_\eta^2$ if the PU is present or not. We assume that in both cases, the value of P is known at each SU. When L is small, the matrix $\mathbf{X}$ of collected samples is what we can call a thin observation matrix and the inherited small size of the covariance matrix $\hat{\mathbf{R}}_{\mathbf{X}}$ eigenvalue calculation requires very few complexity. This last feature is of great importance in the framework of our application.

According to the local spectrum sensing system model, it is obvious that each SU acquires the sensing information through stochastic channel condition, thus each SU indicates its own credibility, and small sample size at each SU increases the uncertainty of observing and reduces the credibility of its sensing. Hence, in order to improve the detection performance and reduce the uncertainty, we propose a new BPA function for evaluating the reliability of each SU in Sect. 3.2. Relying on the new BPA function, D–S fusion rule is used in order to make a final decision in Sect. 3.3.

3.2 Basic Probability Assignment Evaluation

In order to make a final decision by applying D–S theory which allows to combine evidence from different sources and evaluate the credibility of each source with small sample size, we propose a new basic probability assignment function of each SU based on the largest eigenvalue λ_1 of the received sample covariance matrix $\hat{\mathbf{R}}_{\mathbf{X}}$ analysed in Sect. 3.1, which estimates SUs' self-assessed decision credibility. The proposed BPA functions at the ith SU ($i = 1, 2, \ldots, N_{su}$) are based on the integral of the probability density function of the Tracy–Widom distribution of order 1, and are defined as

$$\begin{aligned} m_i(H_0) &= \int_{\lambda_{1i}}^{+\infty} W_1\left(\frac{x-\mu_{0i}}{\sigma_{0i}}\right)\mathrm{d}x \\ &= 1 - F_1\left(\frac{\lambda_{1i}-\mu_{0i}}{\sigma_{0i}}\right) \end{aligned} \tag{25}$$

$$\begin{aligned} m_i(H_1) &= \int_{-\infty}^{\lambda_{1i}} W_1\left(\frac{x-\mu_{1i}}{\sigma_{1i}}\right)\mathrm{d}x \\ &= F_1\left(\frac{\lambda_{1i}-\mu_{1i}}{\sigma_{1i}}\right) \end{aligned} \tag{26}$$

where $m_i(H_0)$, $m_i(H_1)$ are the BPA of hypotheses H_0 and H_1 of the ith SU, which presents respectively credibility for hypotheses H_0 and H_1 to be true. W_1 and F_1 denote the probability density function and the cumulative distribution function for the distribution of Tracy–Widom of order 1 [24, 25]. λ_{1i} is the largest eigenvalue of the received sample covariance matrix $\hat{\mathbf{R}}_{\mathbf{X}}$ of the ith SU. μ_{0i} and σ_{0i} are respectively equal to μ and σ in (23) and (24) with $P = \sigma_\eta^2$. μ_{1i} and σ_{1i} are respectively equal to μ and σ in (23) and (24) with $P = \sigma_s^2 + \sigma_\eta^2$. The third BPA function is

$$m_i(\Omega) = 1 - m_i(H_0) - m_i(H_1) \tag{27}$$

where $\Omega = \{H_1, H_0\}$ denotes that either hypothesis could be true, and $m_i(\Omega)$ is the total uncertainty of the ith SU.

Roughly speaking, if the calculated λ_{1i} turns out to be small, the BPA function $m_i(H_0)$ will get a larger value than $m_i(H_1)$, which will give more credit to the H_0 hypothesis than H_1. Conversely if λ_{1i} is large, the H_1 hypothesis will get a much higher probability than the H_0 hypothesis.

After having evaluated their own BPA and sending them to the FC, this latter will make a final decision by running the D–S based fusion process.

3.3 D–S Fusion and Final Decision

According to D–S theory of evidence and the above new BPA functions (Eqs. (25), (26) and (27)), a new BPA function can be obtained at the FC as follows:

$$m(H_0) = (m_1 \oplus m_2 \oplus \cdots \oplus m_{N_{su}})(H_0) = \frac{1}{1-\kappa} \sum_{\substack{\cap A_i = H_0, A_i \subset 2^{\Omega} \\ i \in \{1,\ldots,N_{su}\}}} \prod_{i=1}^{N_{su}} m_i(A_i) \quad (28)$$

$$m(H_1) = (m_1 \oplus m_2 \oplus \cdots \oplus m_{N_{su}})(H_1) = \frac{1}{1-\kappa} \sum_{\substack{\cap A_i = H_1, A_i \subset 2^{\Omega} \\ i \in \{1,\ldots,N_{su}\}}} \prod_{i=1}^{N_{su}} m_i(A_i) \quad (29)$$

where, in our framework, $2^{\Omega} = \{\emptyset, \{H_0\}, \{H_1\}, \Omega\}$, and κ is a measure of the amount of conflict among the mass sets defined as:

$$\kappa = \sum_{\substack{\cap A_i = \emptyset, A_i \subset 2^{\Omega} \\ i \in \{1,\ldots,N_{su}\}}} \prod_{i=1}^{N_{su}} m_i(A_i) \quad (30)$$

Finally, the decision is made at the FC by simply comparing $m(H_0)$ and $m(H_1)$ as follows:

$$H_1 \text{is true} \quad \text{if } \mathrm{m(H_1) > m(H_0)} \quad (31)$$

$$H_0 \text{is true} \qquad \text{otherwise} \quad (32)$$

4 Simulation Results and Analysis

In the following simulations a captured DTV signal in [26] is considered as the PU signal, with a 0.5 probability of being present. Its center frequency is 545 MHz with a 6 MHz bandwidth. The observed passband signal is frequency-shifted and turned into a baseband signal. It is then sampled at $1/T_s = 100$ KHz rate. This sampling rate is much lower than the 6 MHz bandwidth of the potential PU signal. The channel impulse response duration is set to $T_h = 1\mu s$. In this condition ($T_s > T_h$), collected samples whether a PU is present or not, are totally uncorrelated. With this setting, 0.5 ms is required to collect 50 samples. Channels between the potential PU and the SUs are generated according to the Clark Rayleigh fading model in (5), where the maximum Doppler spread f_D is set to 1000 Hz. The DTV signal parameters and the simulation setup are shown in Table 1. In addition, the additive, white and Gaussian noise (AWGN) channel is considered and it exists a FC which combines evidences from each SU and makes the final decision.

As the first part of simulation, we show the mean behavior of the BPA functions when SNR is varying in Figs. 2 and 3 where the number of sampling is respectively 200 and 50. Since the BPA function of T-DS in [9] is based on the central limit theorem, it is a good estimate of SUs' self-assessed decision credibility only when the number of samples is sufficiently high [13]. Therefore, it is not suitable for the small sample size. According to the Eqs. (25) and (26), we know that $m_i(H_0)$ decreases and $m_i(H_1)$ increases with the

Table 1 DTV signal parameters in [26] and simulation setup

Center frequency	545 MHz
Bandwidth	6 MHz
Sampling period	10 μs
Channel model	Clark model
Channel impulse response duration	1 μs
Maximum doppler spread	1000 Hz
Number of SU	6
Number of PU	1
Number of FC	1

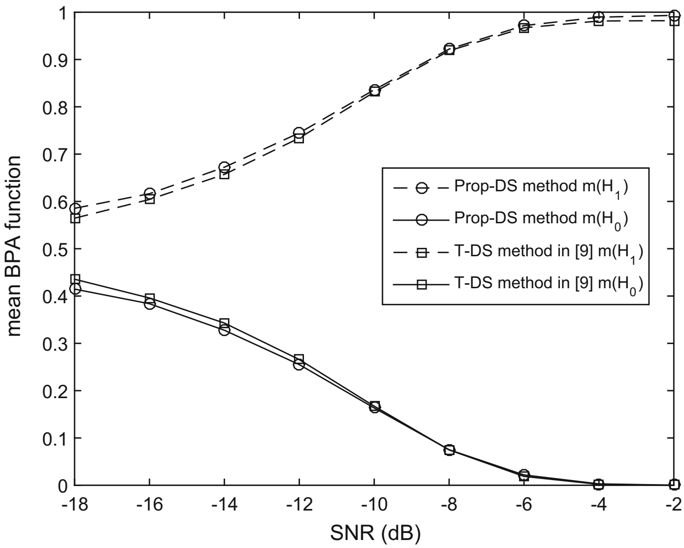

Fig. 2 The variation trend of the BPA functions with the increasing of SNR when PU is present using 200 samples

increasing of the largest eigenvalue λ_{1i} when a PU is present. Then after D–S fusion in (28) and (29), the BPA functions $m(H_0)$ and $m(H_1)$ also should have a declining and increasing trends, respectively. As shown in Fig. 2, when the number of sample is large, i.e. 200 samples, for the proposed method, that is $(N_s, L) = (100, 2)$, the BPA functions in (25) and (26) of the proposed method are very similar to the BPA functions in T-DS [9]. Conversely, when the number of samples is small, the BPA function of the proposed method is still suitable. Figure 3 shows that the BPA functions of the proposed method with small sample size, with 50 samples that is $(N_s, L) = (25, 2)$, has a similar tendency compared to the large sample size, which is not true for T-DS. We can see that the proposed DS (Prop-DS) method has about 5% improvement over T-DS with small sample size. In detail, as shown in Table 2, the improvement of the Prop-DS method is declining with the increasing of the SNR. For example, when the SNR is -14 dB, the mean BPA function $m(H_1)$ of the Prop-DS method and the T-DS method are respectively 0.6534 and 0.5760. Thus, the improvement is 7.74%. While for SNR = -8 dB, the improvement is 4.83%.

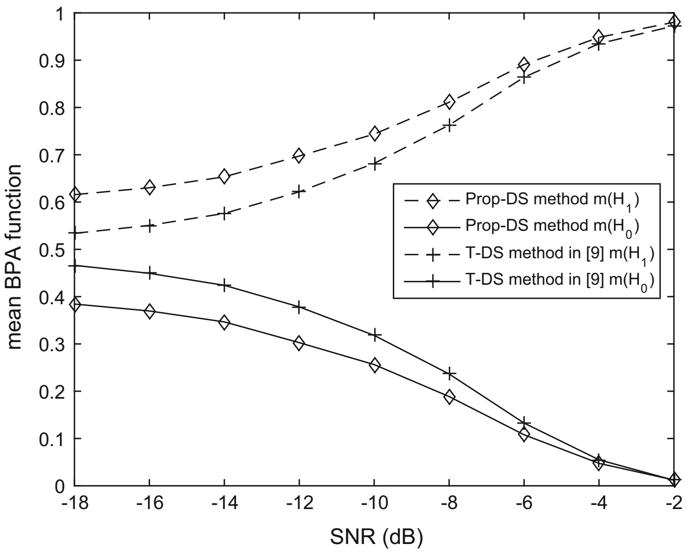

Fig. 3 The variation trend of the BPA functions with the increasing of SNR when PU is present using 50 samples

Table 2 The improvement of the Prop-DS method referring to the mean BPA function

SNR (dB)	−16	−14	−12	−10	−8	−6	−4
Prop-DS ($m(H_1)$)	0.6303	0.6534	0.6973	0.7436	0.8111	0.8908	0.9483
T-DS ($m(H_1)$)	0.5507	0.5760	0.6216	0.6819	0.7628	0.8639	0.9349
Improvement (%)	7.96	7.74	7.57	6.17	4.83	2.69	1.34

Therefore, in order to show the behaviour of the compared methods in a more general scenario, we assume now that each of the six SUs experiences different channel conditions. 100,000 Monte Carlo simulations have been run where SNR at each SU is a random variable with a uniform distribution on the interval [−2, 0 dB]. Based on this setting, Figs. 4 and 5 present the ROC curves of the proposed method and the other methods in [9, 14] and [17]. When the sample number is 200, as shown in Fig. 4, the proposed method (the circular curve) has a litter bit lower detection probability than the maximum-minimum eigenvalue (MME) method in [14] and the eigenvalue-moment-ratio (EMR) method in [17]. As expected when the number of samples is large, the approximated Tracy–Widom distribution is no longer well adapted to characterize the BPA function. This is why the proposed method shows little less attractive performance in that case. Besides with 200 samples, it can be observed that the two eigenvalue-based methods perform much better than the T-DS one. Most importantly, when the sample number is 50, as shown in Fig. 5, it is very obvious that the probability of detection of all methods decline compared with 200 samples. However, the proposed method shows better performance than its counterparts. It can be observed that the ROC curve of the proposed method with 50 samples is even partly above the one of the T-DS method in [9] with 200 samples.

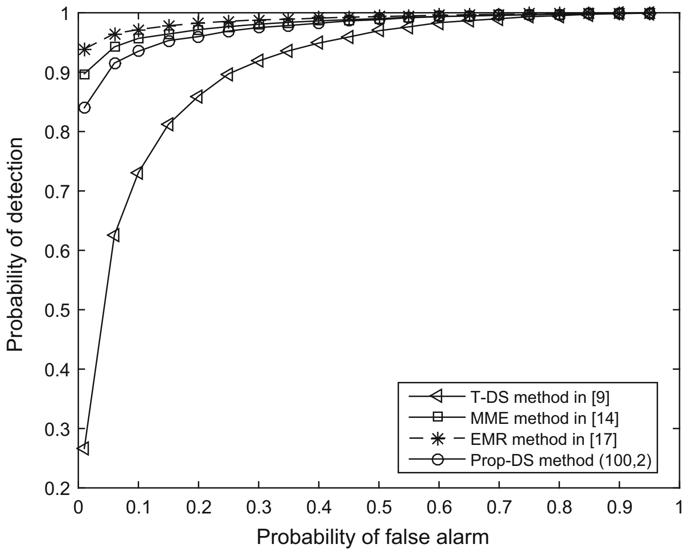

Fig. 4 ROC curves of the compared methods using 200 samples at each SU

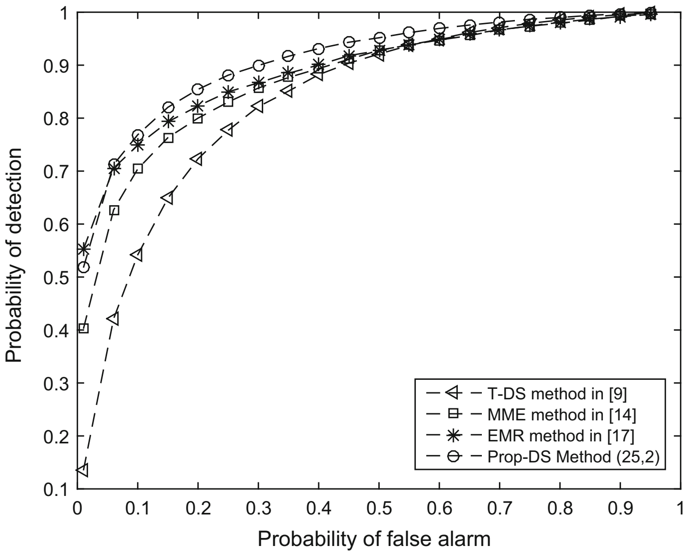

Fig. 5 ROC curves of the compared methods using 50 samples at each SU

In addition, for evaluating the performance of the proposed method with small sample size according to the number of SUs engaged in the process, we show in Fig. 6 the ROC curves of the proposed method when the number of SUs is 10, 8, 6 and 4. The sample size at each SU is 50, and Monte Carlo simulations have been run where the SNR at each SU is randomly chosen in the interval [−20, 0 dB], exactly in the same way as for the Fig. 5. As shown in Fig. 6, the detection performance brings up with the increasing number of SU. When the number of SU is 10, the proposed method can obtain about 0.9 probability of

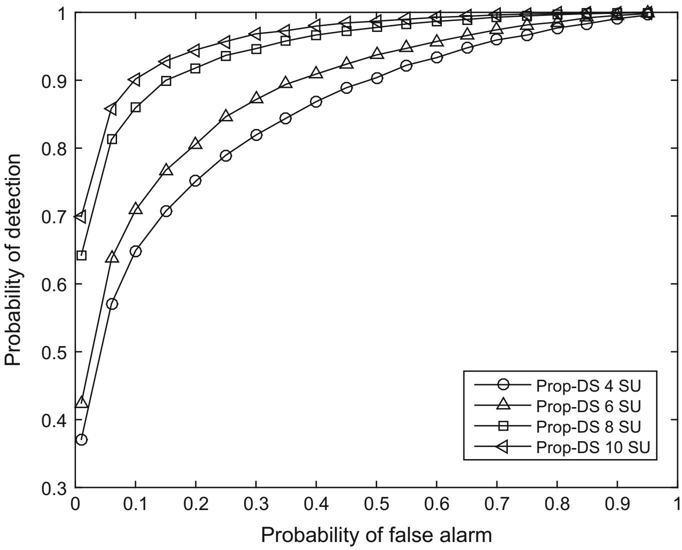

Fig. 6 ROC curves of our proposed scheme with different numbers of SU when the sample number is 50

detection with 0.1 probability of false alarm. And due to the small sample size 50, with $L = 2$, the proposed method keep on exhibiting a very low computational cost, mainly because of the eigenvalue decomposition. It is very suitable in practical CWSNs applications when dealing with constrained power devices.

5 Conclusion

In this paper, cooperative spectrum sensing with small sample size is presented. The advantage of the proposed technique compared to other eigenvalue-based spectrum sensing techniques is that we form a thin observation matrix, which allows to get a small dimension covariance matrix. In that case the eigenvalue decomposition has a negligible cost. Then, a new BPA function is constructed and used in D–S fusion rule, which reduces the conflict of evidence from different SUs. Simulation results have shown that our method can achieve a higher probability of detection than other methods in small sample size situation. In addition, the low computational complexity and the high power efficiency are able to be obtained in our method, which mainly benefits from the small sample size. In the future work, the algorithm in this paper is going to be verified on a hardware platform. Universal Software Radio Peripheral (USRP) and GNU Radio are chosen to implement the evaluation testbed. Besides, taking into consideration more realistic channel model in specific environment, e.g. hotspot, indoor, urban and suburban area, we will explore further robust spectrum sensing algorithm.

References

1. Yücek, T., & Arslan, H. (2009). A survey of spectrum sensing algorithms for cognitive radio applications. *IEEE Communications Surveys & Tutorials*, *11*(1), 116.

2. Sahai, A., Hoven, N., & Tandra, R. (2004). Some fundamental limits on cognitive radio. In *Citeseer 42th Allerton conference on communication, control, and computing*.
3. Urkowitz, H. (1967). Energy detection of unknown deterministic signals. *Proceedings of the IEEE*, *55*(4), 523.
4. Enserink, S., & Cochran, D. (1994). A cyclostationary feature detector. In *IEEE 28th Asilomar conference on signals, systems and computers*, vol. 2, (pp. 806–810).
5. Gavrilovska, L., & Atanasovski, V. (2011). Spectrum sensing framework for cognitive radio networks. *Wireless Personal Communications*, *59*(3), 447.
6. Subhedar, M., & Birajdar, G. (2011). Spectrum sensing techniques in cognitive radio networks: A survey. *International Journal of Next-Generation Networks*, *3*(2), 37.
7. Akan, O. B., Karli, O. B., & Ergul, O. (2009). Cognitive radio sensor networks. *IEEE Network*, *23*(4), 34.
8. Akyildiz, I. F., Lo, B. F., & Balakrishnan, R. (2011). Cooperative spectrum sensing in cognitive radio networks: A survey. *Physical Communication*, *4*(1), 40.
9. Qihang, P., Kun, Z., Jun, W., & Shaoqian, L. (2006). A distributed spectrum sensing scheme based on credibility and evidence theory in cognitive radio context. In *IEEE 17th international symposium on personal, indoor and mobile radio communications (PIMRC)*, (pp. 1–5).
10. Nguyen-Thanh, N., & Koo, I. (2011). Evidence-theory-based cooperative spectrum sensing with efficient quantization method in cognitive radio. *IEEE Transactions on Vehicular Technology*, *60*(1), 185.
11. Han, Y., Chen, Q., & Wang, J.-X. (2012). An enhanced DS theory cooperative spectrum sensing algorithm against SSDF attack. In *IEEE 75th vehicular technology conference (VTC Spring)*. (pp. 1–5).
12. Wang, J., Feng, S., Wu, Q., Zheng, X., Xu, Y., & Ding, G. (2014). A robust cooperative spectrum sensing scheme based on dempster–shafer theory and trustworthiness degree calculation in cognitive radio networks. *EURASIP Journal on Advances in Signal Processing*, *2014*(1), 1.
13. Rugini, L., Banelli, P., & Leus, G. (2013). Small sample size performance of the energy detector. *IEEE Communications Letters*, *17*(9), 1814.
14. Zeng, Y., & Liang, Y.-C. (2009). Eigenvalue-based spectrum sensing algorithms for cognitive radio. *IEEE Transactions on Communications*, *57*(6), 1784.
15. Taherpour, A., Nasiri-Kenari, M., & Gazor, S. (2010). Multiple antenna spectrum sensing in cognitive radios. *IEEE Transactions on Wireless Communications*, *9*(2), 814.
16. Lin, F., Qiu, R. C., Hu, Z., Hou, S., Browning, J. P., & Wicks, M. C. (2012). Generalized fmd detection for spectrum sensing under low signal-to-noise ratio. *IEEE Communications Letters*, *16*(5), 604.
17. Huang, L., Fang, J., Liu, K., & So, H. C. (2015). An eigenvalue-moment-ratio approach to blind spectrum sensing for cognitive radio under sample-starving environment. *IEEE Transactions on Vehicular Technology*, *64*(8), 3465.
18. Ma, Z., et al. (2012). Accuracy of the Tracy–Widom limits for the extreme eigenvalues in white wishart matrices. *Bernoulli*, *18*(1), 322.
19. Cho, Y. S., Kim, J., Yang, W. Y., & Kang, C. G. (2010). *MIMO-OFDM wireless communications with MATLAB*. London: Wiley.
20. Xiao, C., Zheng, Y. R., & Beaulieu, N. C. (2006). Novel sum-of-sinusoids simulation models for rayleigh and rician fading channels. *IEEE Transactions on Wireless Communications*, *5*(12), 3667.
21. Shafer, G., et al. (1976). *A mathematical theory of evidence* (Vol. 1). Princeton: Princeton University Press.
22. Tulino, A. M., & Verdú, S. (2004). *Random matrix theory and wireless communications* (Vol. 1). Hanover, MA: Now Publishers Inc.
23. Johnstone, I. M. (2001). On the distribution of the largest eigenvalue in principal components analysis. *Annals of Statistics, 29*(2), 295–327.
24. Tracy, C. A., & Widom, H. (1996). On orthogonal and symplectic matrix ensembles. *Communications in Mathematical Physics*, *177*(3), 727.
25. Dieng, M. (2005). Distribution functions for edge eigenvalues in orthogonal and symplectic ensembles: Painlevé representations. *International Mathematics Research Notices*, *2005*(37), 2263.
26. Garrison, I., Martin, R. K., Sethares, W. A., Hart, B., Chung, W., Balakrishnan, J., et al. (2001). DTV channel characterization. In *Proceedings of conference on information sciences and systems*.

Shaoyang Men received his B.S. degree in Communication Engineering from Huaqiao University, China, in 2011 and the M.S. degree in Electronics Systems from Polytech'Nantes, Nantes, France, in 2013 and in Communication and Information System from South China University of technology, Guangzhou, China, in 2014. He is currently a Ph.D. student in Digital Communications Systems at Polytech'Nantes (Ecole Polytechnique de l'université de Nantes), Nantes, France. His research interests include cognitive wireless sensor networks, spectrum sensing techniques, resource management and network optimization.

Pascal Chargé is currently full-time Professor at Polytech Nantes (Ecole Polytechnique de l'université de Nantes). His research interests include array signal processing for wireless communications, techniques and technologies for the spectrum sensing, statistical signal processing, and nonlinear dynamical systems. From 2003 to 2010, he has been with the LATTIS Laboratory, University of Toulouse, where he was a Researcher fellow with the Dynamical System Team. Since 2010, he is with the Communication Systems Team of the IETR (UMR CNRS) Laboratory. Since January 2012, Pascal Chargé is also the Head of the Electronic and digital technologies department at the Polytech Nantes Engineering school, University of Nantes.

Sébastien Pillement is a Professor in Polytech'Nantes, France since 2012. He was an associate professor at IUT in Lannion, the subdivision of the University of Rennes 1, during 13 years. He is currently a research member of the SCN Research Team of the IETR Lab. (Research Institute in Electronic and Telecommunication). He received a Ph.D. degree and Habilitation degrees in Computer Science respectively from the University of Montpellier II and the University of Rennes 1. His research interests include dynamically reconfigurable architectures, system on chips, design methodology and NoC (Network on Chip) based circuits. He focuses his research on designing flexible and efficient architectures managed in real-time and on the use of these architectures to increase the reliability of systems. He is the author or coauthor of about 100 journal and conference papers.